Cell Transplantation
Volume 31: 1–11

DOI: 10.1177/09636897221107536
journals.sagepub.com/home/cll
SAGE

Extracellular Vesicles Derived From Hypoxia-Conditioned Adipose-Derived Mesenchymal Stem Cells Enhance Lymphangiogenesis

Yi Yang[1*], Xu-bo Li[1*], Yu Li[1], Tian-xiao Li[2], Ping Li[1], Guang-mao Deng[3], Qiang Guo[3], Xiang Zhou[1], and Xiao-hu Chen[3]

Abstract

Extracellular vesicles from adipose-derived mesenchymal stem cells (ADSCs) play an important role in lymphangiogenesis; however, the underlying mechanisms are not fully understood. In this study, we aimed to investigate the function of extracellular vesicles secreted by hypoxia-conditioned ADSCs in lymphangiogenesis and explore the potential molecular mechanisms. Extracellular vesicles were extracted from ADSCs cultured under hypoxia or normoxia conditions. The uptake of extracellular vesicles by lymphatic endothelial cells (LECs) was detected by immunofluorescence staining. The effects of extracellular vesicles on the viability, migration, and tube formation of LECs were determined by CCK-8 assay, migration assay, and tube formation assay, respectively. Molecules and pathway involved in lymphangiogenesis mediated by ADSC-derived extracellular vesicles were analyzed by luciferase reporter assay, qRT-polymerase chain reaction (PCR), and Western blot. Hypoxia ADSC-derived extracellular vesicles (H-ADSC/evs) significantly enhanced the proliferation, migration, and tube formation of LECs. Hypoxia decreased the expression of miR-129 in ADSC-derived extracellular vesicles. Overexpression of miR-129 counteracted the promoting effect of H-ADSC/evs on lymphangiogenesis. In addition, decreased exosomal miR-129 expression resulted in upregulation of HMGB1 in LECs, which led to AKT activation and lymphangiogenesis enhancement. Our data reveal that extracellular vesicles derived from hypoxia-conditioned ADSCs induce lymphangiogenesis, and this effect is mediated by miR-129/HMGB1/AKT signaling. Our findings imply that hypoxia ADSC-isolated extracellular vesicles may represent as a valuable target for the treatment of diseases associated with lymphatic remodeling.

Keywords

lymphangiogenesis, adipose-derived mesenchymal stem cells, extracellular vesicles, AKT, hypoxia

Introduction

Lymphangiogenesis is a process that forms new lymphatic vessels from pre-existing lymphatic vasculature and plays important roles in many diseases, such as cancer, inflammatory bowel disease, and endometriosis[1–3]. Mesenchymal stem cell (MSC)-based therapy has been considered as a promising strategy for lymphatic regeneration[4], but the underlying mechanism is not fully clarified.

Accumulating evidence suggests that MSCs exert their function via secreting vesicles and molecules[5,6]. Extracellular vesicles are cellular vesicles (40–100 nm in diameter) that are secreted by different types of cells. Extracellular vesicles play an critical function in many processes, such as cell proliferation, survival, migration, apoptosis, immune response, by delivering proteins, mRNAs, or miRNAs from host cells to recipient cells[7,8]. Adipose-derived mesenchymal stem cells (ADSCs) are a population of pluripotent cells derived

[1] Department of Microsurgery, Trauma and Hand Surgery, The First Affiliated Hospital of Sun Yat-sen University, Guangzhou, China
[2] Department of Pharmacy, Hospital of Stomatology, Guanghua School of Stomatology, Sun Yat-sen University, Guangzhou, China
[3] Department of Orthopedic, Huiya Hospital, The First Affiliated Hospital of Sun Yat-sen University, Huizhou, China

* Yi Yang and Xu-bo Li were considered as the first authors since authors contributed equally to this work.

Submitted: January 7, 2022. Revised: May 20, 2022. Accepted: May 31, 2022.

Corresponding Authors:
Xiang Zhou, Department of Microsurgery, Trauma and Hand Surgery, The First Affiliated Hospital of Sun Yat-sen University, Guangzhou 510080, China.
Email: zhoux87@mail.sysu.edu.cn

Xiao-hu Chen, Department of Orthopedic, Huiya Hospital, The First Affiliated Hospital of Sun Yat-sen University, Huizhou 516081, China.
Email: 249004552@qq.com

from adipose tissue, whose characteristics are similar to bone marrow-derived mesenchymal stem cells (BMSCs)[9]. Multiple studies have reported that ADSCs have potential application for promoting lymphatic generation[10–12]. It has been reported that ADSCs promote VEGF-C-dependent lymphangiogenesis via secreting extracellular vesicles[6], indicating that the paracrine effect is critical for ADSC-mediated lymphangiogenesis promotion.

The oxygen concentration is an important factor for stem cell proliferation and differentiation. In the body, the oxygen content is quite low in adipose tissue and thus ADSCs usually exist in low oxygen conditions[13]. Consistently, treatment with hypoxia can promote the proliferation and differentiation of ADSCs and alter their molecule production[14]. However, the function of extracellular vesicles from hypoxia-conditioned ADSCs in lymphangiogenesis remain unclear. In the current study, we investigated the effects of hypoxia ADSC-derived extracellular vesicles on lymphatic endothelial cell proliferation, migration and tube formation, and explored the molecules and pathway involved in this process.

Materials and Methods

Cell Culture

Human ADSCs and dermal lymphatic endothelial cells (LECs) were obtained from Guangzhou Cyagen Biology (Huangpu District, Guangzhou, China). ADSCs were cultured in Dulbecco's Modified Eagle Medium (DMEM) medium (Gibco, Waltham, MA, USA) containing 10% fetal bovine serum (FBS; Gibco, USA) and 1% penicillin-streptomycin (Gibco, USA) under hypoxia (1% O_2) or normoxia conditions (21% O_2). LECs were maintained in endothelial growth medium-2-MV (EGM-2-MV, Lonza) that contains endothelial basal medium-2 (EBM-2, Lonza) and SingleQuots kit (Lonza).

Extracellular Vesicles Isolation

ADSCs were cultured under hypoxia or normoxia conditions for 24 h, and the medium was harvested for extracellular vesicles isolation. The medium was centrifuged at 3,000 g for 15 min and then 20,000 g for 45 min at 4°C. The supernatant was filtered and further centrifuged at 110,000 g for 70 min at 4°C. The sample were washed once with phosphate buffered saline (PBS) and then recentrifuged at 110,000 g for another 70 min at 4°C.

Transmission Electron Microscopy

Extracellular vesicles isolated from ADSCs were resuspended in PBS. A drop of extracellular vesicles was placed on the top of a copper grid. After washing once with PBS, extracellular vesicles were fixed with 3% glutaraldehyde for 15 min. The sample was washed again with PBS and incubated with 2% uranyl acetate for 5 min. Then, exosomes were visualized under a transmission electron microscope. Dynamic light scattering was used to determine the exosome size.

Uptake of Extracellular Vesicles

ADSC-derived extracellular vesicles were labeled with KH67 dye (Sigma, USA). LECs were seeded in 6-well plates and 2 μg KH67-stained extracellular vesicles were added. After incubation for 24 h, LECs were fixed with 4% paraformaldehyde. After stained with DAPI, LECs were analyzed under a confocal microscope (Carl Zeiss, Germany), and the location of extracellular vesicles was visualized.

CCK-8 Assay

LECs (2,000 cells/well) in 100 μl medium were seeded in 96-well plate. For detecting the viability of LECs, 10 μl Cell Counting Kit-8 (CCK-8) reagent (Seyotin, China) was added to each well. After incubation for 1~4 h, the absorbance at 450 nm was determined by a plate reader.

Transwell Migration Assay

LECs (1×10^5) in 100 μl serum-free medium were added into Transwell inserts (Corning, USA), and 600 μl completed medium with 10 μg/ml extracellular vesicles was added to the lower compartment of the chamber. After incubation for 24 h, LECs were fixed with methanol for 10 min and stained with 0.0.5% crystal violet for 15 min. The non-migrating cells were scraped with a cotton swab, and the migrated cells were visualized under an inverted microscope (Carl Zeiss, Germany).

Tube Formation Analysis

Twenty-four-well plates were precoated with Matrigel (BD Sciences, USA) for 30 min at 37°C prior to cell seeding. LECs (2×104 cells/well) were seeded in 24-well plates and 10 μg/ml ADSC-derived extracellular vesicles were added. After incubation for 24 h, the tube number at three random field was counted using a light microscope.

Quantitative RT-PCR

LECs were treated with ADSC-derived extracellular vesicles (10 μg/ml) for 24 h. LECs were collected and used for RNA isolation. Total RNA was extracted using TRIzol reagent (Life Science, Waltham, MA, USA) and was reverse transcribed to cDNA using the PrimeScript RT-PCR kit (Seyotin, China). qPCR was performed with the qPCR Mix (Seyotin, china) on the Applied Biosystems 7300 system (Applied

Biosystems, USA). The experiments were conducted in triplicate. Gene (or miRNA) expression was normalized to GAPDH (or U6) using the $2^{-\Delta\Delta CT}$ formula.

DNA and RNA Transfection

miR-129 mimics and control mimics (NC mimics) were purchased from RiboBio (Guangzhou, China). HMGB1 expression plasmid and control plasmid were obtained from Hanbio (Shanghai, China). miRNA mimics and HMGB1 expression plasmid were transfected into LECs using Lipofectamine 2000 (ThermoFisher, USA) according to the manufacturer's instructions.

Luciferase Reporter Assay

The wild type and mutated HMGB1 3'UTR were cloned into pGL3 plasmid to form recombinant plasmids pGL3-HMGB1-3'UTR-wt and pGL3-HMGB1-3'UTR-mut. LECs (2×105 cells/well) were seeded in 24-well plates and were cotransfected with pGL3-HMGB1-3'UTR-wt (or pGL3-HMGB1-3'UTR-mut), miR-129 mimics (or NC mimics), and pRL-TK (Promega, USA). After transfection for 48 h, the luciferase activity was determined by using a Dual-Luciferase Reporter Assay System (Promega).

Western Blot

LECs or ADSC-derived extracellular vesicles were lysed using RIPA lysis buffer. The sample was separated by SDS-PAGE gel and transferred to PVDF membranes (Millipore, USA). After blocking with 5% non-fat milk, the PVDF membrane was incubated with primary antibody at 4°C overnight. After washing three times with TSB-Tween 20 (TBST), the membrane was incubated with the secondary antibody for 1.5 h at room temperature. After three washes with TBST, the protein bands were detected by using the Western Blot Detection Kit (Seyotin, China). The antibodies used were as follows: CD9 (ab59479; Abcam, UK), CD63 (ab59479; Abcam), TSG-101 (ab125011; Abcam, UK), HMGB1 (ab18256; Abcam, UK), LYVE-1 (ab14917; Abcam, UK), PROX1 (ab101851; Abcam, UK), GAPDH (#2118; Cell Signaling Technology, USA), AKT (#9272; Cell Signaling Technology, USA), and p-AKT (#4060; Cell Signaling Technology, USA).

Statistical Analysis

The data were represented as the mean ± standard deviation (SD) from three independent experiments. Statistical comparisons were performed with Student t-test (two groups) or one-way analysis of variance (ANOVA; more than two groups). A P value lower than 0.05 was considered as statistically significant.

Results

Characterization of Extracellular Vesicles Derived From ADSCs

To identify the potential activity of MSC-derived extracellular vesicles on lymphangiogenesis, exosomes were isolated from ADSCs cultured under hypoxia (H-ADSC/evs) and normoxia conditions (N-ADSC/evs). Transmission electron microscopy and nanoparticle tracking analysis showed that extracellular vesicles were spherical and of 100~150 nm diameter and the morphology and size of H-ADSC/evs and N-ADSC/evs were similar (Fig. 1A, B). To further confirm the extracellular vesicles, the expression of exosomal markers (CD9, CD63, and TSG-101) were analyzed by Western blot. The expression of CD9, CD63, and TSG-101 was detected in both H-ADSC/evs and N-ADSC/evs (Fig. 2C). Next, the internalization of exosomes by LECs were investigated by immunofluorescence staining. The result showed that PKH67-labeled extracellular vesicles could be taken up by LECs (Fig. 1D).

H-ADSC/evs Increases LEC Proliferation, Migration, and Tube Formation

To investigate whether H-ADSC/evs could influence lymphangiogenesis, we detected the effects of H-ADSC/evs on the proliferation, migration, and tube formation in LECs. After treatment with H-ADSC/evs and N-ADSC/evs, the viability of LECs were analyzed by CCK-8. The result showed that H-ADSC/evs significantly increased the viability of LECs compared with N-ADSC/evs (Fig. 2A). Migration assay also showed that treatment with H-ADSC/evs highly elevated the migration activity of LECs compared with N-ADSC/evs (Fig. 2B). In addition, tube number was significantly increased in H-ADSC/evs-treated group compared with the N-ADSC/evs-treated group (Fig. 2C). Moreover, H-ADSC/evs highly increased the mRNA and protein expression of lymphangiogenesis modulators, LYVE-1 and PROX1, compared with N-ADSC/evs (Fig. 2D, E). Together, these data indicate that H-ADSC/evs has a positive effect on LEC proliferation, migration, and tube formation.

Hypoxia-Conditioned ADSC/evs Promote Lymphangiogenesis by Reducing miR-129

Given the important role of miRNAs in lymphangiogenesis, we tested the expression of several miRNAs in extracellular vesicles from ADSCs under hypoxia or normoxia conditions. The result showed that miR-129 was significantly decreased in H-ADSC/evs compared with N-ADSC/evs, while other miRNAs were not altered obviously (Fig. 3A). To access the contribution of miR-129 to H-ADSC/evs-mediated

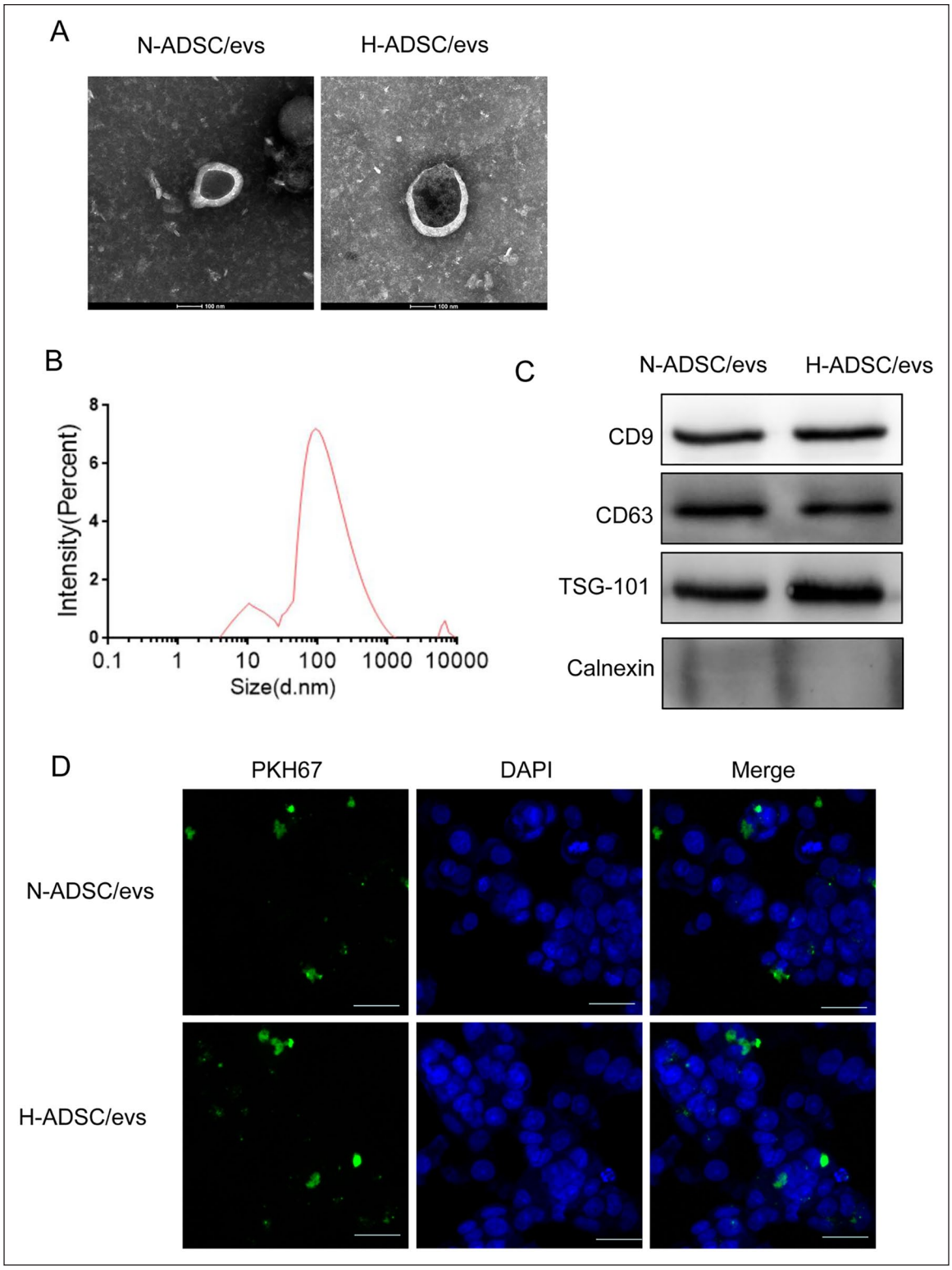

Figure 1. Identification of hypoxia ADSC-derived extracellular vesicles. (A) Transmission electron microscopy analysis of the morphology of H-ADSC/evs and N-ADSC/evs. Scale bars: 100 nm. (B) NTA analysis of H-ADSC/exos and N-ADSC/exos. (C) Western blot analysis of CD9, CD63, and TSG-101 expression in of H-ADSC/evs and N-ADSC/evs. (D) Immunofluorescence staining determining the uptake of hypoxia ADSC-derived extracellular vesicles by LECs. Data represent the mean ± SD of three separate experiments; comparison was performed with Student's *t*-test. Scale bar: 100 μm. ADSCs: adipose-derived mesenchymal stem cells; H-ADSC/evs: hypoxia ADSC-derived extracellular vesicles; LECs: lymphatic endothelial cells; N-ADSC/evs: normoxia ADSC-derived extracellular vesicles; SD: standard deviation.

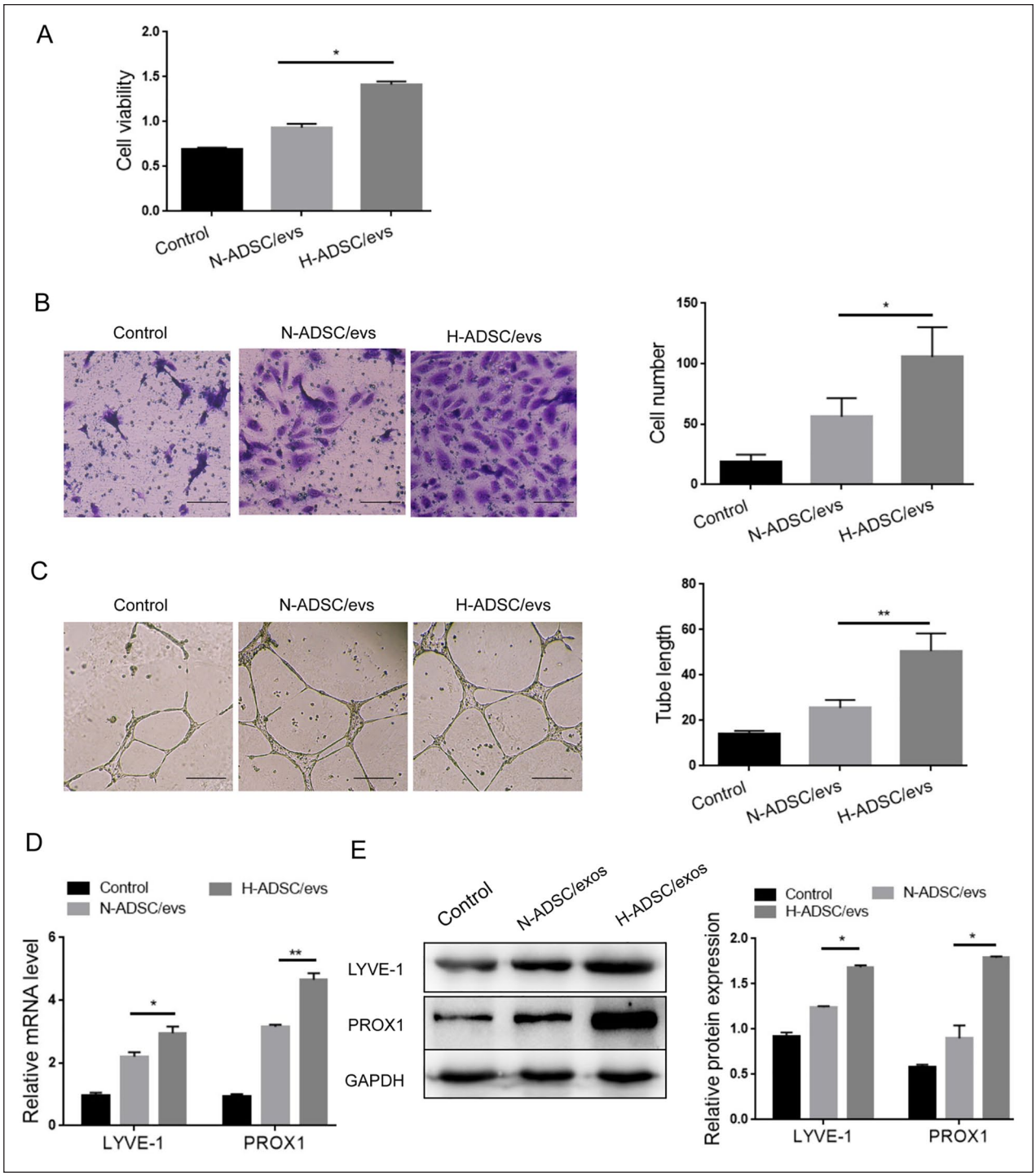

Figure 2. Effects of hypoxia ADSC-derived extracellular vesicles on LEC proliferation, migration, and tube formation.
(A) CCK-8 assay in LECs after treatment with or without H-ADSC/evs (or N-ADSC/evs). (B) Migration assay in LECs after treatment with or without H-ADSC/evs (or N-ADSC/evs). (C) Tube formation assay in LECs after treatment with or without H-ADSC/evs (or N-ADSC/evs). (D, E) qRT-PCR and Western blot analysis of LYVE-1 and PROX1 expression in LECs after treatment with or without H-ADSC/evs (or N-ADSC/evs). *$P < 0.05$, **$P < 0.01$. Data represent the mean ± SD of three separate experiments; comparison was performed with Student's *t*-test. Scale bar: 100 μm. ADSCs: adipose-derived mesenchymal stem cells; CCK-8: Cell Counting Kit-8; H-ADSC/evs: Hypoxia ADSC-derived extracellular vesicles; LECs: lymphatic endothelial cells; N-ADSC/evs: normoxia ADSC-derived extracellular vesicles; mRNA: messenger RNA; SD: standard deviation.

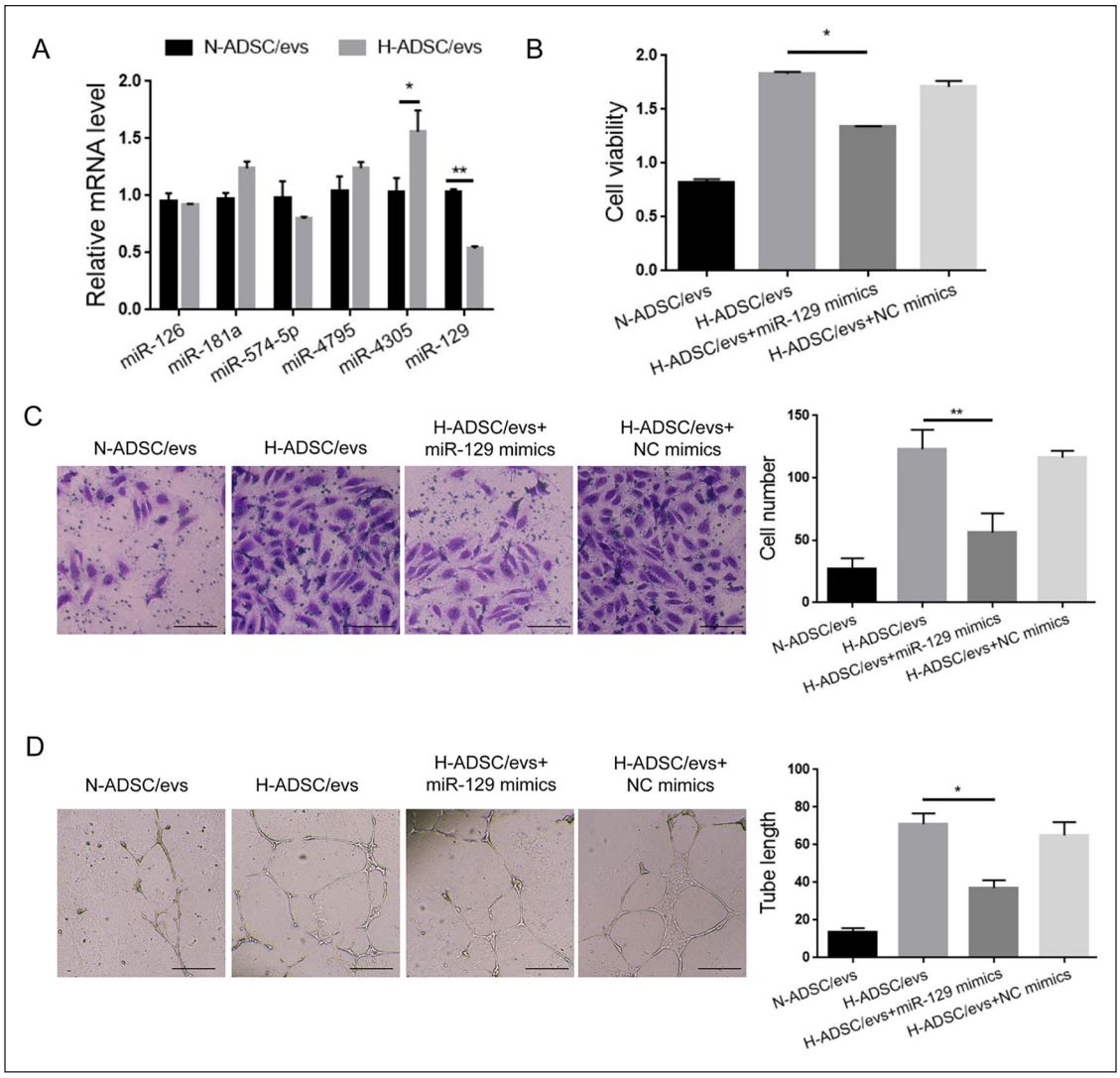

Figure 3. H-ADSC/evs increase lymphangiogenesis by downregulation of miR-129. (A) qRT-PCR analysis of miRNA expression in LECs treated with H-ADSC/evs or N-ADSC/evs. (B) CCK-8 assay in LECs after treatment with H-ADSC/evs (or N-ADSC/evs) together with miR-129 mimics (or NC mimics). (C) Transwell migration assay in LECs after treatment with H-ADSC/evs (or N-ADSC/evs) together with miR-129 mimics (or NC mimics). (D) Tube formation assay in LECs after treatment with H-ADSC/evs (or N-ADSC/evs) together with miR-129 mimics (or NC mimics). Data represent the mean ± SD of three separate experiments; comparison was performed with Student's t-test. Scale bar: 100 μm. ADSCs: adipose-derived mesenchymal stem cells; CCK-8: Cell Counting Kit-8; H-ADSC/evs: Hypoxia ADSC-derived extracellular vesicles; LECs: lymphatic endothelial cells; N-ADSC/evs: normoxia ADSC-derived extracellular vesicles; mRNA: messenger RNA; SD: standard deviation. *$P < 0.05$, **$P < 0.01$.

lymphangiogenesis, we transfected miR-129 mimic to LECs under hypoxia or normoxia conditions before extracellular vesicles extraction. Cell viability analysis and Transwell migration assay showed that treatment with miR-129 decreased the viability and migration of LECs that were increased by H-ADSC/evs (Fig. 3B, C). Additionally, tube formation assay revealed that H-ADSC/evs increased tube formation of LECs, and transfection of miR-129 mimics reversed this effect (Fig. 3D). Collectively, these results suggest that H-ADSC/evs enhances lymphangiogenesis via reduction of miR-129.

miR-129 Suppresses H-ADSC/evs-Mediated Lymphangiogenesis via HMGB1

miRNAs exert their functions usually via modulation of downstream target genes. HMGB1 has been reported to play an important role in lymphangiogenesis and its association with miR-129 has been indicated previously[15]. Our data showed that treatment with H-ADSC/evs increased the expression of HMGB1, and this effect was blocked by overexpression of miR-129 (Fig. 4A). Luciferase reporter assay showed that transfection with miR-129 mimics could reduce

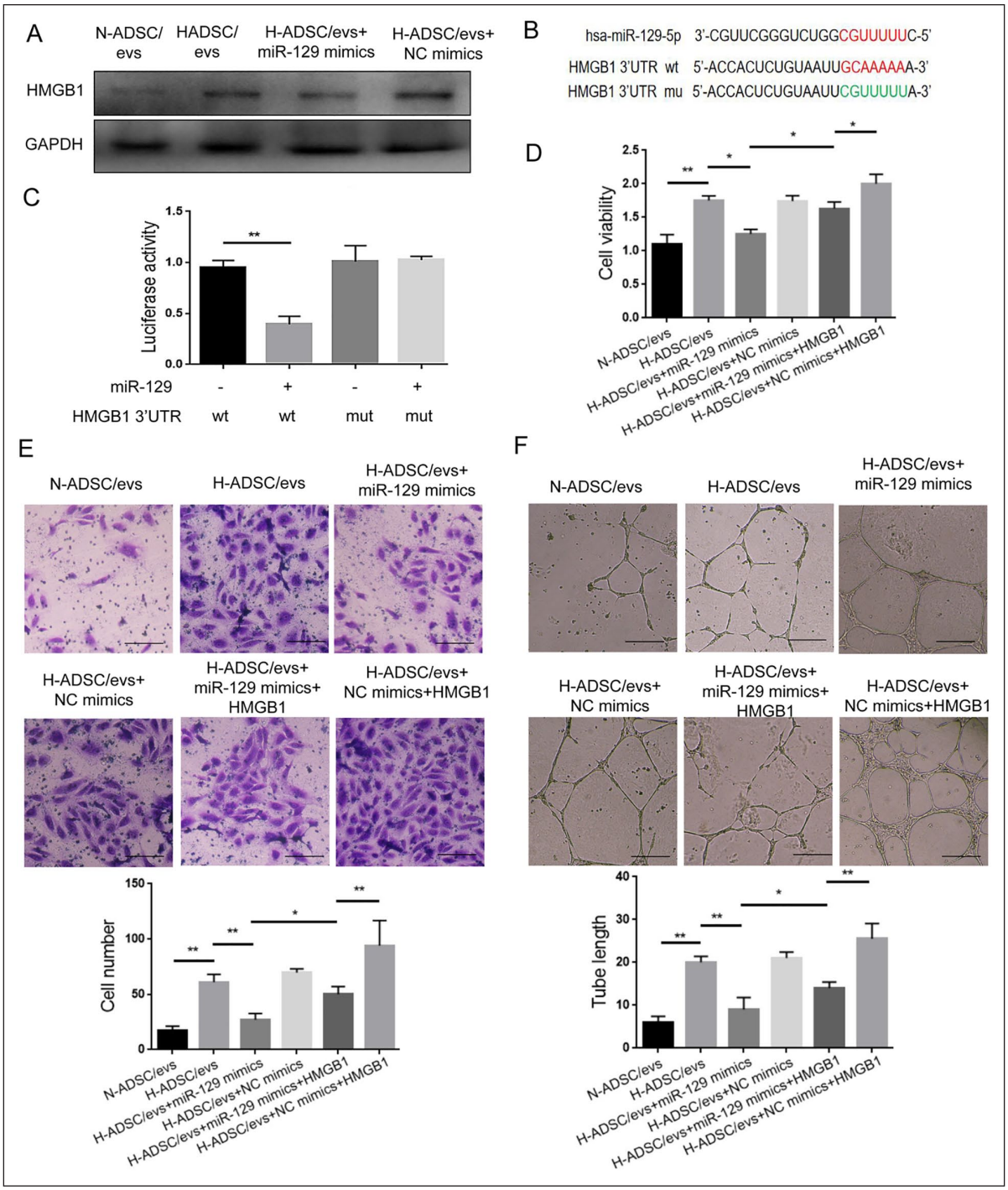

Figure 4. Exosomal miR-129 regulates HMGB1 expression. (A) Western blot analysis of HMGB1 expression in LECs after treatment with H-ADSC/evs with miR-129 mimics or NC mimics. (B) The binding site of miR-129 in HMGB1 3'UTR. (C) Luciferase reporter assay in LECs transfected with miR-129 and wild type (wt) or mutated (mut) HMGB1 3'UTR. (D) CCK-8 assay demonstrated that transfection of miR-129 abolished the effect of H-ADSC/evs on LEC viability, and this effect was reversed by overexpression of HMGB1. (E) Transwell migration assay revealed that transfection of miR-129 mimics counteracted the effect of H-ADSC/evs on LEC migration, and this effect was reversed by overexpression of HMGB1. (F) Tube formation assay showed that overexpression of miR-129 restrained the effect of H-ADSC/evs on LEC tube formation, and this effect was reversed by transfection of HMGB1. Data represent the mean ± SD of three separate experiments; comparison was performed with Student's t-test. Scale bar: 100 μm. ADSCs: adipose-derived mesenchymal stem cells; CCK-8: Cell Counting Kit-8; H-ADSC/evs: Hypoxia ADSC-derived extracellular vesicles; LECs: lymphatic endothelial cells; N-ADSC/evs: normoxia ADSC-derived extracellular vesicles; SD: standard deviation. *$P < 0.05$, **$P < 0.01$.

the luciferase activity of HMGB1 3'UTR, but had no significant effect on HMGB1 3'UTR mutant in LECs (Fig. 4B, C), indicating that HMGB1 is a direct target of miR-129 in LECs. Next, we investigated whether miR-129 inhibited lymphangiogenesis via regulating HMGB1. CCK-8 assay showed that miR-129 suppressed H-ADSC/evs-promoted LEC viability and this effect was reversed by overexpression of HMGB1 (Fig. 4D). Similarly, while miR-129 reduced the migration and tube formation of LECs that were promoted by H-ADSC/evs, ectopic expression of HMGB1 counteracted these effects of miR-129 (Fig. 4E, F). Collectively, these data suggest that H-ADSC/evs promotes lymphangiogenesis via modulating miR-129/HMGB1 cascade.

HMGB1 Induces Lymphangiogenesis via Activation of AKT

To understand the possible pathway by which HMGB1 induced lymphangiogenesis, we tested the expression and phosphorylation of AKT, which is implicated in lymphangiogenesis. Western blot analysis showed that treatment with H-ADSC/evs markedly increased the phosphorylation of AKT, but had no obvious effect on its protein level (Fig. 5A), indicating that H-ADSC/evs could activate AKT signaling. To confirm the involvement of the AKT pathway in H-ADSC/evs-mediated lymphangiogenesis, LECs were treated with AKT inhibitor perifosine. Transwell migration assay showed that H-ADSC/evs increased LEC migration, and treatment with perifosine restrained this promotion (Fig. 5B). Also, administration of perifosine decreased the tube number which was increased by H-ADSC/evs. Taken together, these data indicate that H-ADSC/evs enhances lymphangiogenesis via HMGB1-mediated activation of AKT signaling.

Discussion

Lymphangiogenesis is associated with many critical biological progresses. Increasing reports suggest that MSC-derived extracellular vesicles are potential targets for lymphangiogenesis. However, the underlying mechanisms remain largely unclear. In the present study, we confirmed the promoting effect of extracellular vesicles derived from ADSCs under hypoxia conditions on lymphangiogenesis. Importantly, our results revealed that hypoxia ADSC-derived extracellular vesicles induced lymphangiogenesis via activation of AKT signaling through miR-129/HMGB1 cascade.

A number of miRNAs have been reported to play an important role in lymphangiogenesis[16]. For example, it has been reported that miR-155 promotes lymphatic generation by activating STAT3/VEGFC signaling[17]. MiR-199a/b-5p suppresses lymphangiogenesis by modulating DDR1[18]. miR-129 has been reported to play crucial roles in multiple processes, including cell proliferation, migration, apoptosis, and angiogenesis[19–21]. It has been also reported that miR-129 inhibits lymphangiogenesis in nasopharyngeal cancer via targeting ZIC2[22]. In the present study, we found that the expression of miR-129 was downregulated in H-ADSC/exos-treated LECs compared with N-ADSCs/exos-treated LECs. Moreover, transfection of miR-129 could block the promoting effect of H-ADSC/evs on LEC proliferation, migration, and tube formation. Therefore, our data indicate that the decreased miR-129 expression contributes to H-ADSC/evs-induced lymphatic generation.

HMGB1 is a heparin-binding protein that is involved in many biological processes, such as cell growth, survival, apoptosis, migration, immune response, and so on[23–26]. Mutiple studies have demonstrated that HMGB1 also has an important role in lymphagiogenesis. For instance, it has been reported that curcumin suppresses the lymphangiogenesis of gastric cancer cells via suppression of HMGB1/VEGF-D signaling[27]. Han et al.[28] reported that HMGB1 enhances inflammation-mediated lymphangiogenesis through TLR4-dependent signaling pathway. Li et al.[29] also showed that HMGB1 activates NF-kB to upregulate VEGF-C and thus promotes lymphangiogenesis and lymphatic node metastasis in colon cancer. Consistently, in our study, we found that HMGB1 was a direct target of miR-129 in LECs. Moreover, downregulation of exosomal miR-129 resulted in increased HMGB1 expression in LECs, which consequently led to elevated LEC migration and tube formation.

Accumulating evidence suggests that the AKT-mediated signaling participates in lymphangiogeneis. It has been reported that Qingjie Fuzheng Granule inhibits lymphangiogenesis via the VEGF-C/VEGFR-3-dependent AKT pathway in colorectal cancer[30]. Treatment with human cathelicidin antimicrobial peptide LL-37 enhances lymphangiogenesis in lymphatic endothelial cells through the AKT and ERK signaling pathways[31]. Previous studies have been demonstrated that HMGB1 is an upstream regulator of AKT signaling[32,33]. Here, we found that treatment with H-ADSC/evs increased AKT phosphorylation, and this effect was abolished by HMGB1 silencing. Moreover, treatment with AKT inhibitor perifosine blocked the promoting effects of H-ADSC/evs on LEC migration, as well as the expression levels of LYVE-1 and PROX1. Therefore, HMGB1/AKT signaling is linked to the function of H-ADSC/evs in lymphangiogenesis.

Conclusion

Our results showed that extracellular vesicles secreted by ADSCs cultured under hypoxia conditions have elevating effects on LEC proliferation, migration, and tube formation. Hypoxia reduced the expression of miR-129 in ADSC-derived extracellular vesicles, which led to activation of HMGB1/AKT signaling and thus enhance lymphangiogenesis. Therefore, hypoxia ADSC-secreted extracellular vesicles may serve as a novel strategy for the therapy of lymphangiogenesis-associated diseases.

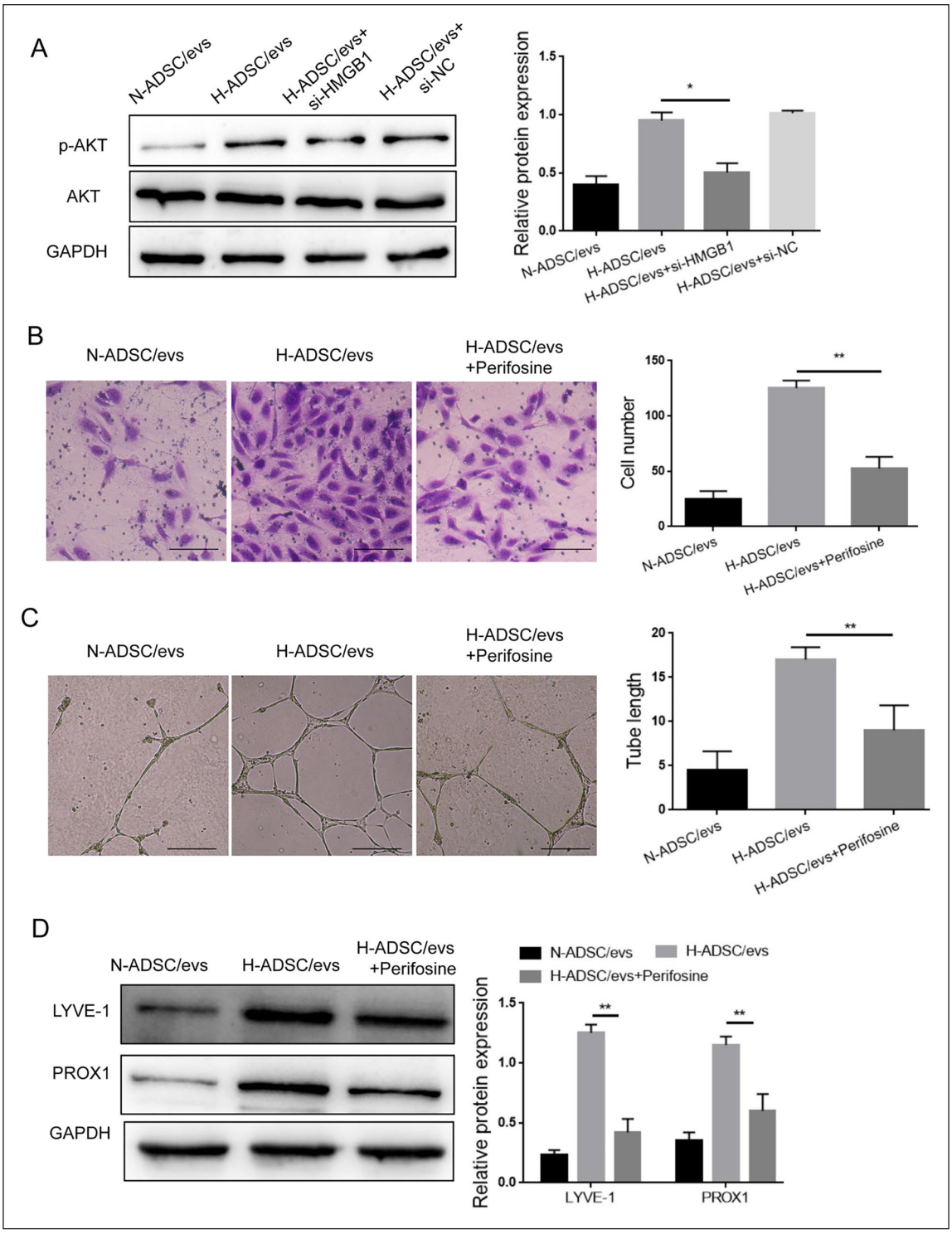

Figure 5. Hypoxia-conditioned ADSC-derived extracellular vesicles activates AKT via HMGB1. (A) Western blot analysis of AKT expression and phosphorylation in LECs after treatment with H-ADSC/evs and transfection with HMGB1 siRNA (si-HMGB1) or control siRNA (si-NC). (B) Treatment with perifosine (30 μM) decreased the tube formation of LECs enhanced by H-ADSC/evs. (D) Treatment with perifosine (30 μM) reduced H-ADSC/evs-induced LYVE-1 and PROX1 expression. Data represent the mean ± SD of three separate experiments; comparison was performed with Student's *t*-test. Scale bar: 100 μm. ADSCs: adipose-derived mesenchymal stem cells; H-ADSC/evs: Hypoxia ADSC-derived extracellular vesicles; LECs: lymphatic endothelial cells; N-ADSC/evs: normoxia ADSC-derived extracellular vesicles; SD: standard deviation. *$P < 0.05$, **$P < 0.01$.

Author Contributions

Yi Yang and Xu-bo designed the experiments and performed the main experiments,Yu Li,Tian-xiao Li,Ping Li,Guang-mao Deng, Qiang Guo, Xiang Zhou analyzed the data, Xiao-hu Chen wrote the manuscript and revised it critically for important intellectual content.

Availability of Data and Materials

For data availability, please contact the corresponding author

Consent for Publication

Agree

Ethical Approval

Not applicable

Statement of Human and animal Rights

Not applicable

Statement of Informed Consent

Not applicable

Declaration of Conflicting Interests

The author(s) declared no potential conflicts of interest with respect to the research, authorship, and/or publication of this article.

Funding

The author(s) disclosed receipt of the following financial support for the research, authorship, and/or publication of this article: This study was supported by the Medical Science and Technology Research Fund project of Guangdong Province (A2020447), National Natural Science Foundation of China (Number 81873530) and Project of Guangdong Provincial Science and Technology Department (2014A010107008).

ORCID iD

Xiao-hu Chen https://orcid.org/0000-0002-9659-2842

References

1. Hattori K, Ito Y, Honda M, Sekiguchi K, Hosono K, Shibuya M, Unno N, Majima M. Lymphangiogenesis induced by vascular endothelial growth factor receptor 1 signaling contributes to the progression of endometriosis in mice. J Pharmacol Sci. 2020;143(4):255–63.
2. Hosono K, Kojo K, Narumiya S, Majima M, Ito Y. Prostaglandin E receptor EP4 stimulates lymphangiogenesis to promote mucosal healing during DSS-induced colitis. Biomed Pharmacother. 2020;128:110264.
3. Hu A, Yang LY, Liang J, Lu D, Zhang JL, Cao FF, Fu JY, Dai WJ, Zhang JF. SIRT2 modulates VEGFD-associated lymphangiogenesis by deacetylating EPAS1 in human head and neck cancer. Mol Carcinog. 2020;59(11):1280–91.
4. Lee CY, Kang JY, Lim S, Ham O, Chang W, Jang DH. Hypoxic conditioned medium from mesenchymal stem cells promotes lymphangiogenesis by regulation of mitochondrial-related proteins. Stem Cell Res Ther. 2016;7:38.
5. Robering JW, Weigand A, Pfuhlmann R, Horch RE, Beier JP, Boos AM. Mesenchymal stem cells promote lymphangiogenic properties of lymphatic endothelial cells. J Cell Mol Med. 2018;22:3740–50.
6. Wang X, Wang H, Cao J, Ye C. Exosomes from adipose-derived stem cells promotes VEGF-C-dependent lymphangiogenesis by regulating miRNA-132/TGF-beta pathway. Cell Physiol Biochem. 2018;49:160–71.
7. Wortzel I, Dror S, Kenific CM, Lyden D. Exosome-mediated metastasis: communication from a distance. Dev Cell. 2019;49: 347–60.
8. He C, Zheng S, Luo Y, Wang B. Exosome theranostics: biology and translational medicine. Theranostics. 2018;8(1):237–55.
9. Kim WS, Park BS, Sung JH, Yang JM, Park SB, Kwak SJ, Park JS. Wound healing effect of adipose-derived stem cells: a critical role of secretory factors on human dermal fibroblasts. J Dermatol Sci. 2007;48(1):15–24.
10. Ahmadzadeh N, Robering JW, Kengelbach-Weigand A, Al- Abboodi M, Beier JP, Horch RE, Boos AM. Human adipose-derived stem cells support lymphangiogenesis in vitro by secretion of lymphangiogenic factors. Exp Cell Res. 2020; 388:111816.
11. Ogino R, Hayashida K, Yamakawa S, Morita E. Adipose-derived stem cells promote intussusceptive lymphangiogenesis by restricting dermal fibrosis in irradiated tissue of mice. Int J Mol Sci. 2020;21:3885.
12. Takeda K, Sowa Y, Nishino K, Itoh K, Fushiki S. Adipose-derived stem cells promote proliferation, migration, and tube formation of lymphatic endothelial cells in vitro by secreting lymphangiogenic factors. Ann Plast Surg. 2015;74(6):728–36.
13. Rochette L, Mazini L, Malka G, Zeller M, Cottin Y, Vergely C. The crosstalk of adipose-derived stem cells (ADSC), oxidative stress, and inflammation in protective and adaptive responses. Int J Mol Sci. 2020;21:9262.
14. Hwang OK, Noh YW, Hong JT, Lee JW. Hypoxia pretreatment promotes chondrocyte differentiation of human adipose-derived stem cells via vascular endothelial growth factor. Tissue Eng Regen Med. 2020;17(3):335–50.
15. Qiu M, Liu D, Fu Q. MiR-129-5p shuttled by human synovial mesenchymal stem cell-derived exosomes relieves IL-1beta induced osteoarthritis via targeting HMGB1. Life Sci. 2021; 269:118987.
16. Jung HM, Hu CT, Fister AM, Davis AE, Castranova D, Pham VN, Price LM, Weinstein BM. MicroRNA-mediated control of developmental lymphangiogenesis. eLife. 2019;8:e46007.
17. Chang Y, Cui M, Fu X, Zhang L, Li X, Li L, Wu J, Sun Z, Zhang X, Li Z, Nan F, et al. MiRNA-155 regulates lymphangiogenesis in natural killer/T-cell lymphoma by targeting BRG1. Cancer Biol Ther. 2019;20(1):31–41.
18. Oh S, Seo M, Choi JS, Joo CK, Lee SK. MiR-199a/b-5p inhibits lymphangiogenesis by targeting discoidin domain receptor 1 in corneal injury. Mol Cells. 2018;41:93–102.
19. Wan P, Bai X, Yang C, He T, Luo L, Wang Y, Fan M, Wang Z, Lu L, Yin Y, Li S, et al. miR-129-5p inhibits proliferation, migration, and invasion in rectal adenocarcinoma cells through targeting E2F7. J Cell Physiol. 2020;235(7–8):5689–701.
20. Li W, Ren Y, Meng T, Yang W, Zhang W. miR-129-5p attenuates hypoxia-induced apoptosis in rat H9c2 cardiomyocytes by activating autophagy. J Gene Med. 2020;22(8):e3200.

21. Zeng A, Yin J, Li Y, Li R, Wang Z, Zhou X, Jin X, Shen F, Yan W, You Y. miR-129-5p targets Wnt5a to block PKC/ERK/NF-kappaB and JNK pathways in glioblastoma. Cell Death Dis. 2018;9:394.
22. Yu D, Han GH, Zhao X, Liu X, Xue K, Wang D, Xu CB. MicroRNA-129-5p suppresses nasopharyngeal carcinoma lymphangiogenesis and lymph node metastasis by targeting ZIC2. Cell Oncol (Dordr). 2020;43(2):249–61.
23. Rouhiainen A, Kuja-Panula J, Wilkman E, Pakkanen J, Stenfors J, Tuominen RK, Lepantalo M, Carpen O, Parkkinen J, Rauvala H. Regulation of monocyte migration by amphoterin (HMGB1). Blood. 2004;104:1174–82.
24. Kuniyasu H, Yano S, Sasaki T, Sasahira T, Sone S, Ohmori H. Colon cancer cell-derived high mobility group 1/amphoterin induces growth inhibition and apoptosis in macrophages. Am J Pathol. 2005;166(3):751–60.
25. Chung H, Nam H, Nguyen-Phuong T, Jang J, Hong SJ, Choi SW, Park SB, Park CG. The blockade of cytoplasmic HMGB1 modulates the autophagy/apoptosis checkpoint in stressed islet beta cells. Biochem Biophys Res Commun. 2021;534:1053–58.
26. Zhang Y, Ren H, Li J, Xue R, Liu H, Zhu Z, Pan C, Lin Y, Hu A, Gou P, Cai J, et al. Elevated HMGB1 expression induced by hepatitis B virus X protein promotes epithelial-mesenchymal transition and angiogenesis through STAT3/miR-34a/NF-kappaB in primary liver cancer. Am J Cancer Res. 2021;11:479–94.
27. Da W, Zhang J, Zhang R, Zhu J. Curcumin inhibits the lymphangiogenesis of gastric cancer cells by inhibiton of HMGB1/VEGF-D signaling. Int J Immunopathol Pharmacol. 2019;33:2058738419861600.
28. Han L, Zhang M, Wang M, Jia J, Zhao M, Fan Y, Li X. High mobility group box-1 promotes inflammation-induced lymphangiogenesis via toll-like receptor 4-dependent signalling pathway. PLoS ONE. 2016;11(4):e0154187.
29. Li Y, He J, Zhong D, Li J, Liang H. High-mobility group box 1 protein activating nuclear factor-kappaB to upregulate vascular endothelial growth factor C is involved in lymphangiogenesis and lymphatic node metastasis in colon cancer. J Int Med Res. 2015;43:494–505.
30. Huang B, Lu Y, Gui M, Guan J, Lin M, Zhao J, Mao Q, Lin J. Qingjie Fuzheng Granule suppresses lymphangiogenesis in colorectal cancer via the VEGF-C/VEGFR-3 dependent PI3K/AKT pathway. Biomed Pharmacother. 2021;137:111331.
31. Yanagisawa T, Ishii M, Takahashi M, Fujishima K, Nishimura M. Human cathelicidin antimicrobial peptide LL-37 promotes lymphangiogenesis in lymphatic endothelial cells through the ERK and Akt signaling pathways. Mol Biol Rep. 2020;47(9):6841–54.
32. Meng L, Li L, Lu S, Li K, Su Z, Wang Y, Fan X, Li X, Zhao G. The protective effect of dexmedetomidine on LPS-induced acute lung injury through the HMGB1-mediated TLR4/NF-kappaB and PI3K/Akt/mTOR pathways. Mol Immunol. 2018;94:7–17.
33. Lv X, Zhu Y, Deng Y, Zhang S, Zhang Q, Zhao B, Li G. Glycyrrhizin improved autophagy flux via HMGB1-dependent Akt/mTOR signaling pathway to prevent Doxorubicin-induced cardiotoxicity. Toxicology. 2020;441:152508.